CRAB CAVITIES

R. Calaga, R. De-Maria (BNL), E. Metral, Y. Sun, R. Tomás, F. Zimmermann (CERN)

Abstract

With lower betas at collision points or longer bunches, luminosity loss due to the crossing angle becomes important. Crab cavities could minimize the loss. The scenarios for a crab crossing implementation in the LHC, the expected performance gain, hardware implications, R&D plan is presented. Some aspects related to machine protection, collimation, aperture constraints, impedance, noise effects to ensure safe beam operation with crab cavities are also addressed.

INTRODUCTION

Operating at the beam-beam limit, the luminosity upgrade of the LHC is foreseen to follow two main paths:

- Lattice modification: Simultaneous reduction of β^* at the collision point and the Piwinski angle via crab crossing [1].
- Beam current: Significant increase in bunch intensities beyond the nominal intensities (x1.5-5) [3] or/and a reduction of beam emittances (x2 or smaller).

Although, significant challenges confront both path, the final upgrade is likely to exploit a combination of the two. Table 1 shows some relevant parameters for the nominal and subsequent upgrade of the LHC.

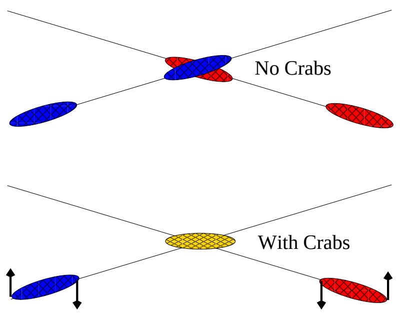

Figure 1: Concept of crab crossing scheme using RF cavities to maximize the bunch overlap at the collision points.

The reduction of β^* below nominal is attractive and technically feasible but the presence of the parasitic interactions requires a proportional increase of the crossing angle. Therefore, the full potential of a β^* reduction can only be realized by recovering the geometric loss of the crossing angle either via crab compensation scheme or an early

Table 1: Some relevant parameters for the LHC nominal and upgrade lattices.

	Unit	Nominal	Upgrade
Energy	[TeV]	3-7	7
P/Bunch	[10^{11}]	1.15	1.7
Bunch Spacing	[ns]	50-25	25
ϵ_n (x,y)	[μm]	3.75	1.0-3.75
σ_z (rms)	[cm]	7.55	7.55
IP$_{1,5}$ β^*	[m]	0.55	0.14-0.25
Betatron Tunes	-	{64.31, 59.32}	
Piwinski Angle	$\frac{\theta_c \sigma_z}{(2\sigma^*)}$	0.64	0.75
BB Parameter, ξ	per/ip	0.003	0.005
X-Angle: θ_c	[mrad]	0.3	0.5
Main RF	[MHz]	0.4	0.4
Crab RF	[GHz]	0.4	0.4
Peak luminosity	[10^{34} $cm^{-2}s^{-1}$]	1.0	3-5

separation scheme [4]. In addition, the crab cavities offer a natural luminosity leveling knob to maximize the integrated luminosity and the lifetime of the IR magnets due to radiation damage [5].

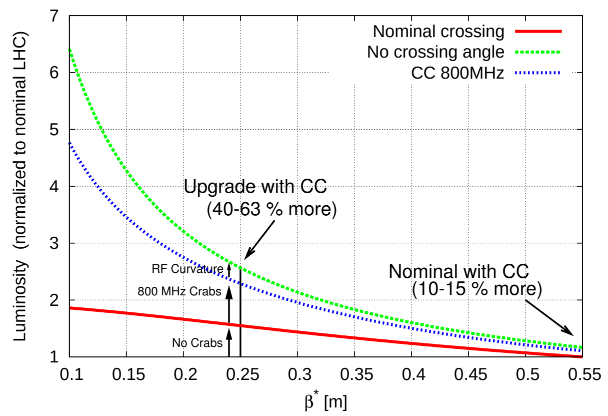

Figure 2: Peak luminosity gain as a function of β^*. The effect of the constant separation for parasitic interactions is taken into account.

The luminosities independent of an intensity upgrade are listed in Table 2 for different operational scenarios of the LHC. The cavity voltage required for each scenario can be calculated using

$$V_{crab} = \frac{2cE_0 \tan(\theta_c/2)\sin(\mu_x/2)}{\omega_{RF}\sqrt{\beta_{crab}\beta^*}\cos(\psi^x_{cc\to ip} - \mu_x/2)} \quad (1)$$

where E_0 is the beam energy, ω_{RF} is the RF frequency of the cavity, β_{crab} and β^* are the beta-functions at the cavity and the IP respectively, $\psi^x_{cc\to ip}$ is the phase advance from the cavity to the IP and μ_x is the betatron tune. A voltage of ~5 MV (single cavity) will suffice with a β_{crab} of 3-5 km and a local scheme with optimum phase advance.

Table 2: Operational scenarios for different β^* and collision energies in the LHC. The required cavity voltage depends on the final optics and placement of the crab cavities with respect to the IP. The integrated luminosity assumes a run time of 10 hr/store, turn-around-time of 5 hrs and a total run time of 220 days.

β^* [m]	θ_c [μrad]	E_b [TeV]	L/L$_0$ [%]	Int L/yr
0.25	439	7.0	63%	22%
0.30	401	7.0	40%	19%
0.55	296	7.0	10%	NE
10.0	273	0.45	0.12%	NE

LHC BOUNDARY CONDITIONS

Superconducting RF is the technology choice to reach required high transverse kick voltages. Although the exact cavity voltage depends on the final optics of the upgrade, a typical kick gradient of ~5 MV is required for some scenarios. This gradient corresponds to a factor of 8 (or 20) in surface electric (or magnetic) fields in a conventional elliptical cavity [8]. Due to physical dimensions and technological constraints, higher frequencies (0.5-1.5 GHz) are generally preferred.

The LHC poses two main boundary conditions for the implementation of crab crossing:

- Long bunches of 7.55 cm ($1\sigma_z$) which confines the maximum RF frequency to 800 MHz. The effect of 800 MHz RF curvature is depicted in Fig. 3 which translates to reduction in luminosity compared to linear kick. Therefore, lower frequencies are preferred (for example: 400 MHz).
- Beam-to-beam separation of 194 mm along the 27 km with a few exceptions like the IR4 region.

A conventional elliptical cavity at 800 MHz radially measures at ~250 mm making it incompatible in most of the ring. Therefore, a new design with a compact footprint is essential (see Table 3).

POSSIBLE SCHEMES

Three crab crossing schemes can be conceived for the LHC considering only the high luminosity interaction points.

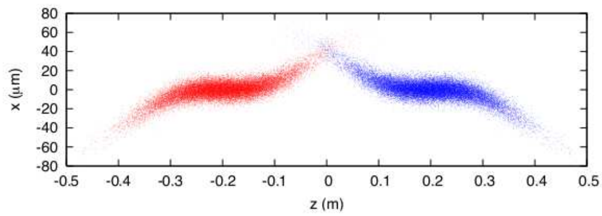

Figure 3: Imperfect overlap of crabbed bunches at the collision point due to curvature of an 800 MHz RF cavity (graphic courtesy K. Ohmi).

- A global scheme with a minimum of one cavity per beam placed in IR4 dogleg region. The IR4 region has the advantage of larger beam-to-beam separation (see Table 3) than the rest of the ring allowing room for conventional technology [2]. However, this scheme poses extreme constraints on the possible phase advance between IP1 and IP5 and on the crossing scheme.
- A less constrained global scheme can be implemented with two cavities per beam. However, an additional dog-leg in another straight section is required.
- A flexible option without phase advance and crossing angle constraints can easily be implemented via local scheme at each IP. This requires new crab cavity concepts to fit within the IR region constraints (see Table 3).

Table 3: Aperture specifications for the IR4 dog-leg region for the global scheme and IR1 and IR5 high luminosity regions for a local scheme.

	Magnet	Aper-H [mm]	B1-B2 sep [mm]	Outer, R [mm]	L [m]
IR$_4$	D$_3$	69	420	395	9.45
	Crabs	84	220-300	195	10
	D$_4$, Q$_5$	73	194	169	15.5
IR$_{1,5}$	D$_1$	134	-	-	10
	Crabs	84	194	150	10
	D$_2$	69	-	-	10

IMPEDANCE & RF TECHNOLOGY

The LHC impedance is dominated by the numerous collimators [6] but additional impedance (both narrow band and broadband) from sources like crab cavities need to be minimized. Tolerances can be set by estimating the impedance requirements from Refs. [7, **?**]. HOM damping is defined by the 200 MHz RF system at 450 GeV to 60 kΩ. This is reduced to 10 kΩ for upgrade intensities (1.7×10^{11} p/bunch). It is estimated that single and coupled-bunch

Table 4: Frequencies, R/Q's and HOM damping requirements for the two-cell elliptical cavity based on impedance tolerances.

Mode Type	Frequency [GHz]	R/Q [Ω]	Q_{ext}
Monopole	0.54	35.2	∼10-100
	0.69	194.5	
Deflecting	0.80	117.3	10^6
Dipole	0.81	0.46	∼100-1000
	0.89	93.4	
	0.90	6.79	

longitudinal modes above 2 GHz will be Landau-damped due to the frequency spread of synchrotron oscillations. In the transverse plane the impedance threshold is given as 2.5 MΩ/m by the damping time of 60 ms at 450 GeV for nominal intensity. For upgrade intensities this is reduced to 0.8 MΩ/m. An additional factor of $\beta/\langle\beta\rangle$ is needed to account for the local β-funtion. The natural frequency spread, chromaticity, bunch-by-bunch transverse damper and Landau octupoles should also damp potentially unstable modes above 2 GHz.

A two-cell elliptical cavity at 800 MHz was developed as a baseline structure. The nominal voltage for the two-cell cavity was set at 2.5 MV to allow for additional margin on peak surface fields. Due to tight tolerances on narrow band impedances, the cavity modes need to strongly damped (see Table 4). Therefore, special coupler designs targeted at specific modes were developed (see Fig. 4) [9]. Alternative damping designs were also developed for the two-cell design to meet the damping specifications [10, 11].

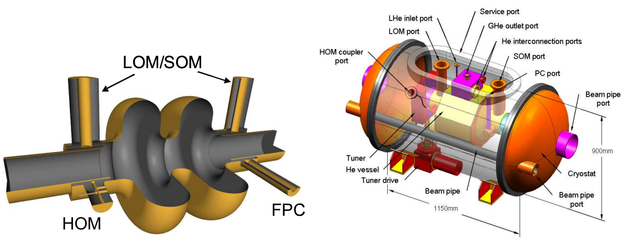

Figure 4: Schematic of the two cell elliptical LHC crab cavity [9] and cryostat [2].

A conceptual design of the cryostat was also developed for the two-cell baseline cavity-coupler to satisfy the IR4 beam line configuration (see Fig. 4. A modular structure was adapted for additional cavities if needed. The helium box contains interconnection ports for the second cavity. A service port is suggested for the He inlet/outlet ports as well as for the RF couplers (main, LOM and SOM). The outer diameter is constrained by the limited space between Helium vessel and cryogenic line. A design of the main power coupler which is nominally oriented in the horizontal plane requires a vertical output due to beam line configuration. The horizontal length of the coupler is limited to ∼150 mm. A possible solution is a T-connection similar to the KEK Tristan-type ERL coupler [12].

COMPACT CAVITIES

As a crab scheme local to the collision points offer the most flexibility in optics and crossing scheme, deflecting structures with a compact footprint (see Fig. 5) are required.

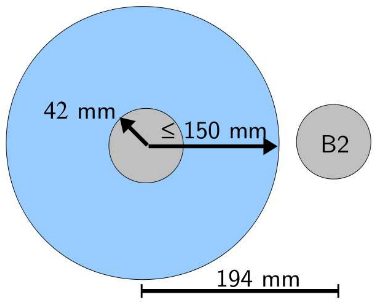

Figure 5: Schematic of the beam pipe separation in the LHC beam lines.

The effort to compress the cavity footprint recently resulted in several TEM type deflecting mode geometries. Apart from being significantly smaller than its elliptical counterpart, the deflecting mode is the primary mode thus giving paving way to a new class of cavities at lower frequencies (400 MHz) which is preferred from the RF curvature point of view (see Fig. 6).

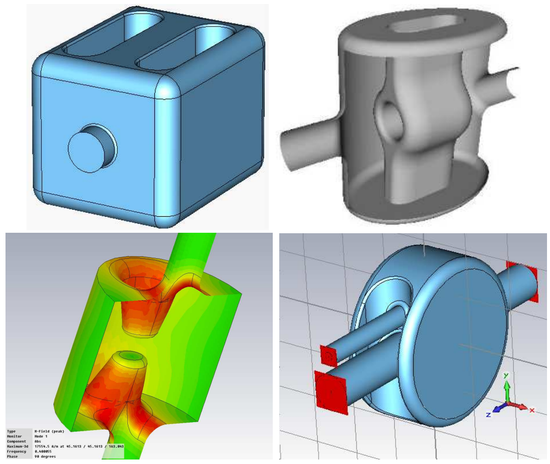

Figure 6: Top left: Half wave double rod cavity [13]. Top right: Half wave single rod cavity [14]. Bottom left: Double rod loaded cavity [10]. Bottom right: Rotated pill-box Kota cavity [11].

The ratio of the kick gradient to the peak surface fields for some designs are lower by a factor of 2 or more than the elliptical counterpart. Therefore, one may theoretically expect a kick voltage also larger by a factor of 2, assuming the surface field limitations are similar to elliptical cavities. These cavities also have the added advantage of large separation in frequency between the deflecting mode and other higher order modes. Therefore, HOM damping becomes simpler. Nevertheless, the coupler concepts developed for the elliptical design are being adapted to achieve the similar level of damping in the compact cavities. Prototypes of some compact designs are underway to validate the RF properties.

MACHINE PROTECTION & COLLIMATION

Due to the immense stored energy in the LHC beams at 7 TeV (350 MJ), protection of the accelerator and related components is critical. For example, at nominal intensity and 7 TeV, 5% of a single bunch is beyond the damage threshold of the superconducting magnets [15]. Approximately, 200 interlocks with varying time constants ensure a safe transport of the beam from the SPS to the LHC and maintain safe circulating beams in the LHC. A worst case scenario for detecting an abnormal beam condition is 40 μs ($\frac{1}{2}$ a turn), and the corresponding response time to safely extract the beams is about 3 turns (see Fig. 7).

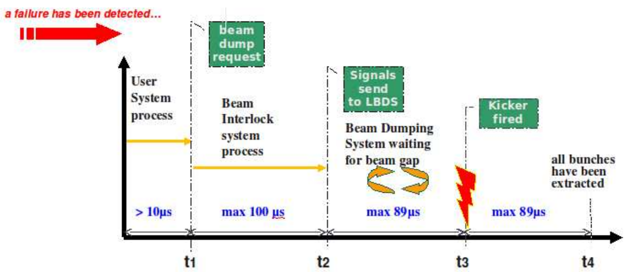

Figure 7: Sequence of a failure detection and full beam extraction [**?**].

Crab cavity failures can abruptly change particle trajectories and induce unwanted beam losses. Some failure scenarios are:

- Single turn failures caused due to sudden cavity quench, power amplifier trips, abrupt RF phase changes and other potential causes.
- Slow failures caused by vacuum degradation, IR cavity to cavity voltage and phase drifts and others.

Any crab cavity related failure must fall under the shadow of the 3-turn extraction time. The high Q_{ext} could favor a slow voltage ramp down, but the voltage slope can be strongly driven by the beam. Therefore, active feedback is essential to guarantee machine protection [18]. Detailed tracking studies are needed to confirm the local and global loss maps in case of abnormal failure scenarios.

Collimation efficiency is a serious concern for LHC beams. The impact on collimation with the existing collimators setup in IR3 and IR7 is minimal for a local scheme. For a global scheme, studies were carried out with a single crab cavity placed in the IR4 region to achieve head-on collisions at IP5 [17]. As a non-adiabatic increase in crab cavity kick results in emittance growth, the cavity voltage is ramped over 1000 turns after which the collimators are input in the tracking simulations. Results show no observable difference in the loss maps between nominal LHC and that with global crab cavities (see Fig. 8).

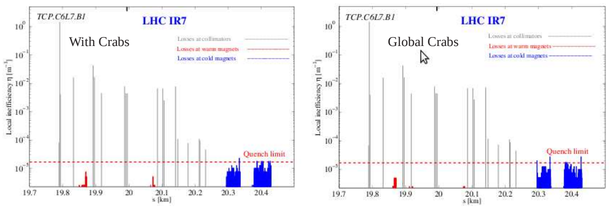

Figure 8: Loss maps around the LHC ring (left) for the nominal LHC and nominal LHC with a global crab scheme (right).

The impact parameters (physical distance to the edge of a collimator) are listed in Table 5 for the globally crabbed beam and compared to the nominal LHC case. A typical value of 1-2μm is used for nominal beam (on-momentum particle) based on diffusion studies. The impact parameters for the crabbed beam in the 1^{st} turn are about a factor of 5 higher. However, for off-momentum particles, the impact parameters are similar to the nominal case and hence the effective cleaning inefficiency remains similar.

Table 5: Impact parameters and particles absorbed on the primary collimator TCP.C6L7.B1 at IR7 with on-momentum (top) and off-momentum (bottom) from tracking 5×10^6 particles.

	Nominal		Crab Cavity	
	$2\sigma_z$	$3\sigma_z$	$2\sigma_z$	$3\sigma_z$
1^{st} turn [μm]	0.78	0.78	3.84	3.84
All turns [μm]	0.153	0.154	0.147	0.147
Part. absorbed.	70.2%	70.2%	68.5%	68.5%
1^{st} turn [μm]	50.61	59.82	76.16	79.03
All turns [μm]	36.1	40.44	66.47	67.03
Part. absorbed	96.5%	97%	99.56%	99.56%

In addition, the hierarchy of the collimator family needs to be maintained for efficient cleaning. To properly account for lattice dispersion and crab dispersion, an effective amplitude function is defined as

$$A_z = \sqrt{\delta_p^2 + \delta_z^2}. \quad (2)$$

A phase space cut of all collimators was constructed as a function of the effective δ_p (with δ_z set as $1\sigma_z$) in the presence of crab cavities to determine the allowed region for beam. The constructed phase cut is similar to the one of the nominal LHC and maintains the hierarchy of the primary, secondary and tertiary collimators critical for efficient collimation.

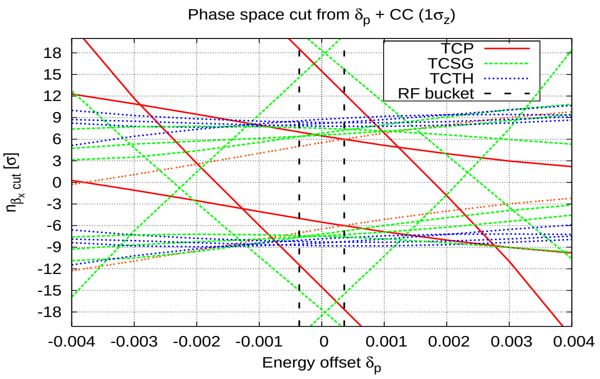

Figure 9: Phase space cut of all the collimators in the LHC with crabbed beams. The hierarchy of the primary (red), secondary (green) and tertiary (blue) collimators

Dynamic aperture studies were also carried out and no significant impact was visible. A maximum decrease of 1σ was calculated for the global crab crossing scheme (nominal DA 13σ). In addition suppression of synchro-betatron resonances was clearly visible.

PHASE NOISE & KEK EXPERIMENTS

Measurements at KEK-B show the side bands of the RF spectrum due to modulated phase noise at frequencies from 50 Hz to 32 kHz. This phase noise leads to dynamic offsets at the collision point and related emittance growth with higher frequencies being more dangerous [1]:

$$\Delta x_{ip} = \frac{c\theta}{\omega_{RF}}\delta\phi \quad (3)$$

$$\frac{\Delta\epsilon}{\Delta t} \propto \frac{\xi^2}{\beta^*}\Delta x_{ip}^2. \quad (4)$$

Noise studies were carried which consisted of scanning the RF phase noise in the CCs and measure the corresponding beam size blow-up. Figure 10 summarizes the scans on the two rings (LER and HER) at frequencies close to the horizontal betatron tunes. The first visible effects occur at about -60dB for both rings without beam-beam. This corresponds to about 0.1° RF phase noise. Similar scans were carried out with the beams in collision and observing the luminosity in the Belle experiment (see Fig. 10). The luminosity is recorded as a function of RF phase noise while exciting the LER and HER CCs individually. First visible effects appear at -70dB, which corresponds to about 0.03°. This value can be extrapolated to the LHC CC tolerances as a high ceiling, i.e. the LHC cavity phase noise must be smaller than 0.03° since the radiation damping in LHC is almost negligible.

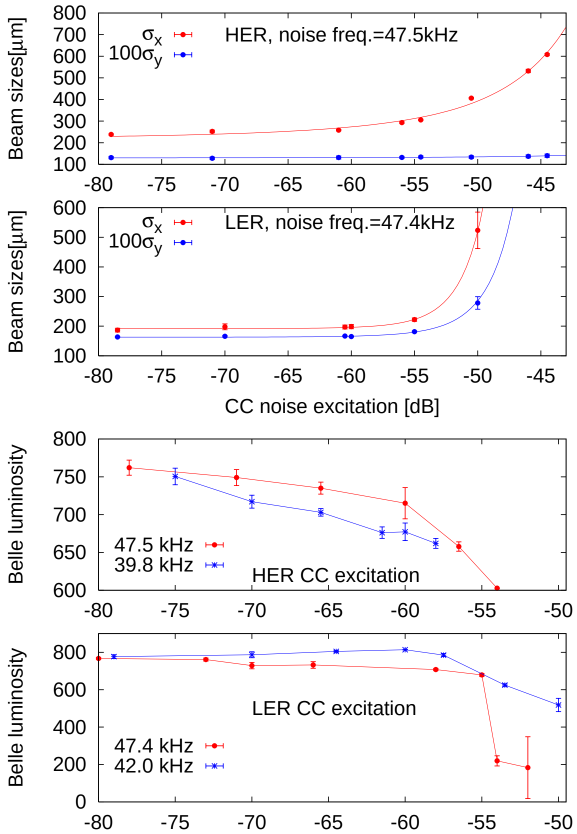

Figure 10: Top: Beam size versus RF phase noise when exciting the LER and HER CCs individually (no beam-beam). Bottom: Luminosities measured at the BELLE detector as a function RF phase noise amplitude at two different frequencies in the presence of beam-beam.

Strong-strong beam-beam simulations (3D) were carried out to study phase noise effects and emittance growth of colliding beams with a local crab compensation at IP_5 in the LHC (β*=0.25m, θ_c=0.522 mrad). The simulations were performed with 2.5 million macro-particles per beam, a 128×128 transverse grid, and 10 longitudinal slices. with a 400 MHz local crab scheme. These simulations indicate a tolerance of $0.02\sigma\tau$ for 10% emittance growth per hour, where σ is the transverse offset and τ is the correlation time This is approximately consistent with KEK-B experiments. Weak-strong simulations with a phase error at varying frequencies observed from the KEK-B cavities were performed. For the highest frequencies (32 kHz), the resulting dynamic offset collisions yield a tolerance of $\leq 0.1\sigma$ to control the emittance growth below 10% per hour. With the low-level RF technology it should be feasible to meet the tolerances but more simulations are needed to accurately define the specifications. It should be noted that the phase noise tolerances will be additionally relaxed due to luminosity leveling as the crab voltage maybe smallest when the beam-beam parameter is at a peak.

OPERATIONAL ISSUES

During regular operation, it is mandatory for the crab cavities to be invisible during injection and magnetic ramp cycle. The cavity will be nominally detuned from the resonant frequency to stay invisible to the beam unless when needed. The high-beta optics and "zero-voltage" in the crab cavities should additionally minimize any perturbation to the beam. As injection oscillations are inevitable, a controlled orbit feedback system to keep the beam offsets small ($< 500\mu$m) will be in place. Active feedback to compensate any beam loading with the RF amplifier will also be mandatory.

At top energy, the cavity is re-tuned and adiabatically ramped to the maximum voltage to avoid any emittance growth. If luminosity leveling is required, the cavity voltage will be ramped as a function of a pre-determined run time to optimize integrated luminosity for the experiments. To operate beyond the beam-beam limit, a scheme with a fully anti-crabbed ($2\theta_c$) to fully crabbed beam during a physics store can be implemented. However, phase noise issues should be studied to ensure minimal emittance growth due to such a scheme. In addition the beams must be fully anti-crabbed before collision bumps are removed. Some luminosity gain estimates are listed in Table **??** for an LHC beam with crab cavities.

From an operational view, a vertical by-pass (see Fig. 11) can minimize a prolonged shutdown and maintenance due to any failures related to crab cavity infrastructure.

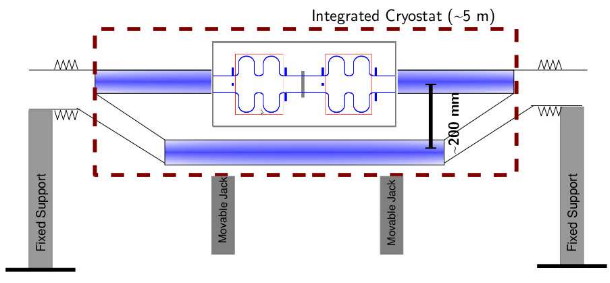

Figure 11: Vertical bypass to raise the crab cavities into the beam-line with the aid of precision motors. Bellows at either end will allow for safely removing the cavities out of the LHC beam-line when not needed.

LHC-CC09 & FUTURE

The 3rd workshop on LHC crab cavities (LHC-CC09) resulted in a conclusive R&D path towards a future implementation of crab crossing in the LHC. The technical challenge of crab implementation and open issues related to hadron beams with crab crossing calls for

- Compact cavities for a local scheme compatible with LHC constrains
- Possible test in another hadron machine (for example: SPS) to identify the differences between electrons and protons.

SPS lends itself as an ideal test bench to study the effects of crab cavities on hadron beams. Other hadron machines of interest are the Tevatron and RHIC where tests may not be extremely relevant for the LHC [21]. A working group identified several aspects including integration, cryogenics, infrastructure and feasibility of a test in the SPS [22]. No show stoppers were found and the possibility of using KEK-B crab cavities in the SPS can be realized at the end of 2012. Fig. 12 shows the optics near the LSS4 region currently hosting the COLDEX experiment. This region has a horizontal bypass which where the experiment can be moved in when needed. Such a setup is ideal for crab cavity tests if the cryostat can be integrated into the current spacial configuration. The KEK-B crab cavities can be integrated with some difficulty but precise civil engineering details need to be worked out to install and precisely move a 5-ton object including cryogenics and RF power.

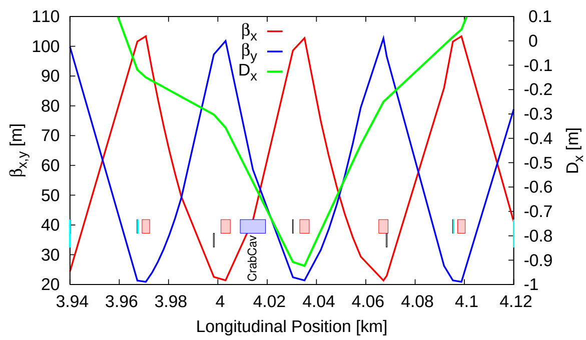

Figure 12: Optics in the LSS4 section near the COLDEX region which can potentially host the test crab cavities in the SPS.

Tracking studies have been launched to study various aspects of the tests in the SPS. Fig. 13 shows first turn trajectories of $1\sigma_z$ particle as a function of longitudinal position. Two collimators TCSP.51934 and a proposed test collimator from SLAC are positioned such that one collimator sees maximum excursion while the other with almost minimum orbit deviation. This setup can aid in beam halo studies and impact on the collimator jaws. Although, intra-orbit deviation can be easily detected via the existing head-tail monitor which has sub-millimeter resolution. If KEK-B cavities become available for an SPS test, a retuned cavity to 511 MHz could be tested with a 100 ns bunch spacing at 55 GeV to perform lifetime studies. Other bunch configurations like 25 and 50 ns can be interesting to test bunch by bunch variations with crab cavities. An active RF feedback will be needed during the SPS enery ramp as the dynamic tuning of the frequency is limited to 1kHz/sec.

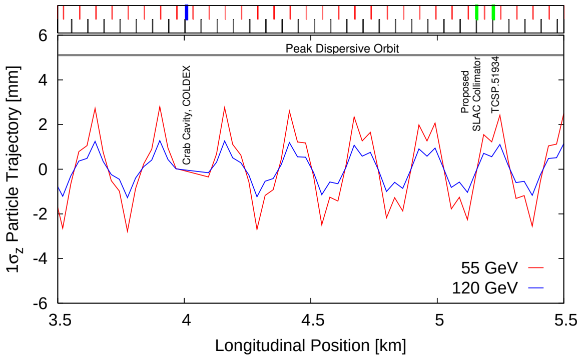

Figure 13: First turn trajectories of a particle at $1\sigma_z$ near the LSS4 region. Two collimators placed upstream are with the right phase advance to see zero and maximum orbit deviation respectively.

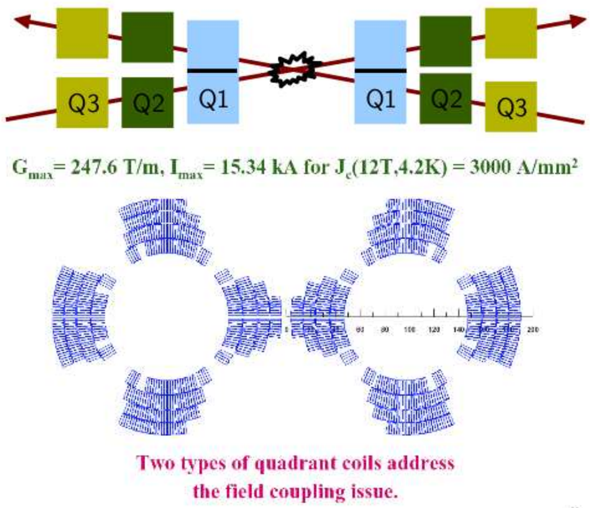

Figure 14: Common yoke separated coils for Q_1 followed by separated focusing channel. This magnet design assumes Nb_3Sn technology for the focusing triplets.

Machine protection studies pertinent to the LHC will be studied to determine different type of interlocks based on RF (fast) and orbit (slow) measurements. Cavity failure scenarios such as cavity trips, abrupt RF voltage and phase changes and related effects on the beam will be studied. General operational aspects such as adiabatic voltage ramping, cavity transparency and other issues are also of interest.

If crab crossing is successfully implemented in the LHC, a future upgrade can potentially increase the crossing angle to accommodate a common yoke separated coil for the Q_1 focusing magnet followed by a separated focusing channel as depicted in Fig. 14. A magnetic design for such configuration with a large aperture ($\sim$100 mm) and high gradient already exists. Field coupling between the two apertures are resolved by two types of quadrant design [23]. This configuration will alleviate long range beam-beam issues which is one of the limitations for the upgrade of the LHC. Considerable flexibility can be realized in IR optics to go beyond any current limitations. However, this geometry will require crossing angles of 4-5 mrad making the upgrade to solely rely on crab crossing. Use of flat beams is preferred to reduce the geometric loss due to crossing angle.

ACKNOWLEDGMENTS

We would like to thank all the members of LHC-CC collaboration for valuable discussions and their contributions. We would like to extend a special thanks to R. Assmann, J.-P. Koutchouk, J. Tuckmantel, N. Solyak, V. Yakovlev, J.R. Delayen, Y. Funakoshi, N. Kota, Y. Morita, G. Burt, B. Hall, P .A. McIntosh, Z. Li, L. Xiao for their contribution to the LHC crab cavity studies.

REFERENCES

[1] R. Calaga et al.,CARE-HHH 2008, Chavannes-de-Bogis.

[2] R. Calaga et al., LHC crab cavities; R. Calaga et al., LHC crab cavity cryostat, in the proceedings of PAC09, Vancouver, Canada, 2009.

[3] F. Zimmermann et al., LHC performance workshop, Chamonix, 2010.

[4] J.-P. Koutchouk and G. Sterbini, An Early Beam Separation Scheme for the LHC Luminosity Upgrade, EPAC06 Proceedings, Edinburgh.

[5] J.-P. Koutchouk et al., LHC performance workshop, Chamonix, 2010.

[6] E. Métral et al., LHC project report 1015.

[7] E. Shaposhnikova, LHC Project Note 242 (2000); F. Sacherer, IEEE Tr. Nucl.Sci. NS-20 , 825 (1973); V. Balbekov et al., IHEP Preprint 91-14, Protvino (1991).

[8] K. Hosoyama et al., in the proceedings of EPAC08, Genoa, Italy, 2008.

[9] L. Xiao et al., in the proceedings of PAC09, Vancouver, Canada, 2009 (3517).

[10] B. Hall et al., in the proceedings of PAC09, Vancouver, Canada, 2009 (2398).

[11] N. Kota, presented at the LHC-CC09 workshop, CERN, Geneva, 2009.

[12] H. Sakai, et al, ERL07, Daresbury Laboratory, Warrington, UK, May 21-25, 2007.

[13] J. Delayen et al., presented at the LHC-CC09, CERN, Geneva, 2009.

[14] Z. Li, presented at CM13, Port Jefferson, NY, 2009.

[15] R. Schmidt et al., in the proceedings of PAC07, Albuquerque, NM, 2007.

[16] J. Wenninger, presented at the LHC-CC09, CERN, Geneva, 2009.

[17] Y. Sun et al., PRST-AB, 12, 101002 (2009).

[18] J. Tuckmantel, private communication.

[19] K. Ohmi, Beam-beam effect with an external noise in LHC, in the proceedings of PAC09, Vancouver, Canada, 2009.

[20] R. Tomás et al., to be submitted to PRST-AB.

[21] R. Calaga, F. Zimmermann, LHC test justification note, *https://twiki.cern.ch/twiki/bin/view/Main/LHCCrabCavities*.

[22] http://emetral.web.cern.ch/emetral/CCinS/CCinS.htm.

[23] A. Kashikin (Not pubished); R. Gupta, private communication. R. Tomas et al., ”Crab cavity optics with 8mrad crossing angle”, proceedings of LUMI 06.